Computational and Experimental NMR Definition of Differences in the Conformational Behavior of Free and Lectin-Bound Glycomimetic Aza/Carba-Lactosides

María del Carmen Fernández-Alonso,[a] F. Javier Cañada,[a] Dolores Solís,[b] Xuhong Cheng,[c] Govindaraj Kumaran,[c] Sabine André,[d] Hans-Christian Siebert,[d] David R. Mootoo,[c] Hans-Joachim Gabius,[d] and Jesús Jiménez-Barbero*[a]

Keywords: Agglutinin / Azasugars / C-disaccharide / Drug design / Glycomimetics / Lectin

Versatile synthetic procedures make saccharide derivatives with substitution at various sites available. Because of the particular involvement of galactosides in biorecognition processes, with lectins affecting growth regulation and adhesion, lactose has become a popular starting point for systematic structure variation. Since shape and flexibility are key parameters for ligand binding, we studied the conformational behavior of aza/carba-C/O analogues of lactose (compound **1**, aza-C; compound **2**, carba-O). Computational calculations and NMR spectroscopy revealed conspicuous differences between **1** and **2** in the extents of accessible conformational area and flexibility. The aza-C derivative also revealed clear shifts in population density relative to lactose, attributable to the *exo*-anomeric effect. The assumption that the derivatives can act as glycomimetics was substantiated by binding studies with a plant lectin. The aza-C analogue **1** maintained a higher degree of flexibility when bound than the O-glycosidically linked carbadisaccharide **2**. The experimental detection of exclusive NOEs characteristic of different conformers of bound **1** [i.e., H1′/H4 (*syn*-Φ), H1′/H3 (*anti*-Ψ), and H2′/H4 (*anti*-Φ) NOE cross-peaks] argues in favor of the ligand still harboring a certain degree of flexibility when bound to mistletoe lectin (VAA). In contrast, there is unambiguous evidence for binding of the major *exo*-anomeric conformer of **2** by VAA, as indicated by the presence of the exclusive NOE of H7eq′/H4. Evidently, structural variations between closely related compounds can translate into clear differences in the lectin-bound states of glycomimetics.

Introduction

The emergence of insights into the functionality of the sugar code has taught an important lesson: the interaction between oligosaccharides from cellular glycoconjugates and lectins is involved in diverse processes from fertilization and differentiation to cell migration and routing, as well as in growth regulation, with relevance for medical applications in drug delivery and growth control.[1] Equally notably, the pathogenesis of bacterial and viral infections often starts with an initial protein−carbohydrate contact, and so the production of clinically effective anti-adhesion reagents based on the carbohydrate target epitopes has become an attractive goal. In this context, the custom-made design of carbohydrates or glycomimetics with improved affinity, pharmacodynamic properties, or synthetic availability is considered to be a promising research field in drug development.[2] One focus of research has been directed towards the substitution of *endo*- or *exo*-glycosidic oxygen atoms by methylene groups in order to confer increased resistance to hydrolytic degradation as an aid for prolonged serum availability when used as drug.[3] With the synthesis of C- and carbaglycosides mastered, the issue as to whether these compounds can serve as "true" mimetics in terms of the crucial factor of shape needs to be properly addressed. Ideally, substitution should not impair the delicate enthalpic/entropic contribution to the free enthalpy change on the thermodynamic balance sheet but might even offer room for affinity enhancement.[4]

Since the substitution of these oxygen atoms by methylene groups evidently results in changes in both the size and the electronic properties of the glycosidic linkages, the flexibility and the energy barriers to rotation around the interresidual linkages would be expected to change to some extent,[5] particularly in the anomeric effects.[6] The conse-

[a] Centro de Investigaciones Biológicas, CSIC, Ramiro de Maeztu 9, 28040 Madrid, Spain
E-mail: jjbarbero@cib.csic.es
[b] Instituto de Química Física Rocasolano, CSIC, Serrano 117, 28009 Madrid, Spain
[c] Department of Chemistry, Hunter College CUNY, 695 Park Avenue, New York, NY 10021, USA
[d] Institut für Physiologische Chemie, Tierärztliche Fakultät, Ludwig-Maximilians-Universität München, Veterinärstr. 13, 80539 München, Germany
Supporting information for this article is available on the WWW under http://www.eurjoc.org or from the author.

  DOI: 10.1002/ejoc.200300679

quences of such variation for intermolecular interactions are largely unknown, prompting this investigation. Here, in continuation of our previous reports, particularly on C-glycosyl and carbaglycosyl compounds, we report a conformational study of the lactose analogues presented in Figure 1, when free in solution. Having accomplished this analysis, we next answer the questions as to whether and to what extent the conformational aspects of the free compounds are influenced when the analogues are bound to a lectin, with the toxic lectin from mistletoe [*Viscum album* agglutinin (VAA) or viscumin] as the model. This lectin has been chosen for its remarkable biological activity spectrum triggered by galactose-specific binding, demonstrating the important role of galactosides in biorecognition also known from animal lectins.[7] At the cellular level, ligand binding at low lectin concentrations stimulates growth of immune and tumor cells, while it is essential for import into the cell at high concentrations, a prerequisite for exerting toxicity intracellularly through the A-chain's enzymatic activity as rRNA glycosidase is similar to the infamous biohazard ricin.[7c,8]

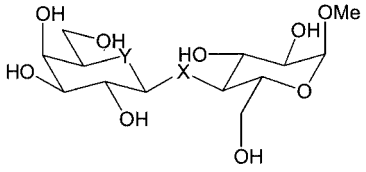

1: Y = NH X = CH_2
2: Y = CH_2 X = O
3: Y = O X = O
4: Y = O X = CH_2

Figure 1. Schematic view of compounds **1** and **2**, and comparison with lactose (**3**) and C-lactose (**4**)

The technique we have used is based on a combination of NMR spectroscopy and molecular mechanics (MM) and molecular dynamics (MD) calculations. This approach has proven its value in delineation of the conformational properties of C-glycosides.[9] To pinpoint differences with respect to lactose (compound **3**) and its C-analogue **4** we followed this strategy with compound **1** and **2**.

Results and Discussion

Molecular Mechanics and Molecular Dynamics Calculations for the Synthetic Compounds

The potential energy surfaces of both synthetic compounds were calculated by use of the MM3*[10] and AMBER*[11] force-fields, as described previously.[12] The GB/SA solvent model for water was used, since the combination of this with these two force-fields has been shown to provide satisfactory matches for the conformational properties of saccharides.[12,13] These maps are useful for delimiting the low-energy regions accessible through rotation around the glycosidic torsion angles Φ and Ψ (Table 1). As shown in Figure 2, calculations by use of the MM3* force-field predict that compounds **1** and **2** should have distinct conformational behavior patterns.

Five low-energy conformers are calculated for compound **1**, in marked contrast with lactose (**3**), for which a prevailing and two minor conformations have been shown to coexist in solution[13] (see Figure 1 in the Supporting Information; for Supporting Information see also the footnote on the first page of this article). They are: A) *exo*-Φ/Ψ_+, B) non-*exo*-Φ/Ψ_-, C) *exo*-Φ/Ψ_-, D) *exo*-Φ/*anti*-Ψ, and E) *anti*-Φ/Ψ. Only four conformers (A, B, D, and E) are stable for compound **2**. According to the calculations based on the MM3* force-field, the most densely populated area in the energy map of compound **1** is C, the *exo*-Φ/Ψ_- conformer (see Table 1 in the Supporting Information). For compound **2**, in contrast, the most frequently occurring conformer is A, populating the *exo*-Φ/Ψ_+ region. The relative energy values calculated by AMBER are fairly similar to those described above (Table 1 in the Supporting Information). The fairly similar sets of predictions from calculations with the two different force-fields are of note with respect to the controversy relating to the optimal choice of proper force-fields when dealing with sugar molecules.[14] To enable detailed structural comparison of the defined structures, the key geometric features (torsion angles and H−H distances) of the conformers A−E of compounds **1** and **2** are listed in Tables 1 and 2, respectively.

Importantly, a number of key proton−proton short distances (< 3 Å) show up only in one of the different conformers. They are generally referred to as *exclusive contacts*. The presence of corresponding signals in NOE spectra (see below) is thus as characteristic as a fingerprint for the presence of the corresponding conformer in the conformational equilibrium. In short, for **1**, these exclusive contacts are HproS−H3 (conformer A), H1′−H4 (conformer B and C), H1′−H3, HproR−H6a, and H1′−H5 (conformer D), and H2′−H4 (conformer E). In the case of **2**, the exclusive NOEs are H1′−H6 (depending on the gg/gt rotamer) and H7′eq−H4 (conformer A). For conformer B, there are no exclusive short distances, but with distances being slightly above 3 Å the pairs H7′eq-H3 and H1′-H3 establish such contacts; *anti*-type conformers D and E also have exclusive NOEs: the contact H7′eq−H5 for D and the contact H7′ax−H4for E.

The conformational stabilities of the different conformers of **1** and **2** were examined computationally by MD simulations[15] with both the MM3* and AMBER* (data not shown) force-fields, and also with the GB/SA explicit solvent model. The computed Φ/Ψ distributions for both **1** and **2** are illustrated in Figure 3, while the distance histogram and average distances of several key H−H interproton distances that appear to be related to observed NOEs (see below) are shown in Figure 2 in the Supporting Information, and in Tables 1 and 2, for **1** and **2**, respectively.

The numeric values of these distances, along with their expected NOEs, calculated by a full relaxation matrix approach, are also presented in Tables 1 and 2.

Table 1. Expected distances estimated from the molecular mechanics (MM) and molecular dynamics simulations (MD) for the two low-energy conformers for compound **1**; the range is the result of the MM3* and AMBER* calculations; the key distances and NOEs are given in bold-italic; collected average distances together with the calculated NOEs based on a full-matrix relaxation approach in comparison with the intensities of the observed NOEs are also given

Proton pair	H−H distances from MM3* and AMBER* molecularmechanics calculations for single conformers					Average H−H distances from MM3* molecular mechanics (MM) and dynamics calculations (MD)		Observed NOES in comparison to those estimated from MM and MD calculations (MM3*) according to a full-matrix relaxation approach		
	(A)	(B)	(C)	(D)	(E) Ψ	Ensemble average (MM)	MD	NOEs from MM3	NOEs from MD	Observed NOE intensity[a]
	exo-Φ/Ψ$_+$	Non-*exo*-Φ/Ψ$_-$	*exo*-Φ/Ψ$_-$	Φ/*anti*-Ψ	*anti*-Φ/eclipsed-Ψ					
H1′−H3	4.5−4.6	3.3−3.7	4.3−3.9	2.0−2.3	4.9−4.7	3.4	3.7	1.4%	1.2%	+
H1′−H4	3.4−3.5	2.1−2.4	2.4−2.5	3.8−3.7	3.7	2.6	2.5	6.2%	6.9%	++++
H1′−H5	3.1−3.2	4.6	4.6−4.7	2.7−2.3	4.7−4.8	3.9	4.2	0.5%	0.3%	+
H1′−H6a	2.0−2.1	5.0−4.5	4.2−4.6	4.0−3.4	3.9	2.9	2.9	1.8%	1.5%	+++
H2′−H4	4.2−4.3	3.3−3.8	4.7−4.6	4.8−4.6	2.8−2.2	3.6	3.9	0.6%	0.4%	+
H3−HR	2.8−2.9	2.4−2.3	2.4−2.6	3.8	2.4	2.5	2.4	5.9%	6.1%	+++
H3−HS	2.5−2.6	3.7−3.5	3.6−3.8	3.1−3.2	3.3−3.2	3.3	3.2	0.7%	0.9%	+
H5−HR	3.7−3.8	2.6−2.9	2.7−2.5	3.2−3.3	3.2−3.3	2.7	2.9	1.8%	1.2%	+++
H5−HS	2.5−2.6	2.9−2.7	2.7−3.0	3.85	2.5	2.7	2.6	1.6%	1.8%	++
HR−6a	4.1−4.2	3.3−3.6	3.4−3.0	2.3−2.2	3.4	3.4	3.4	0.6%	0.6%	+

[a] Intensities are shown as: very weak but significant (+), weak (++), medium (+++), strong (++++), very strong (+++++).

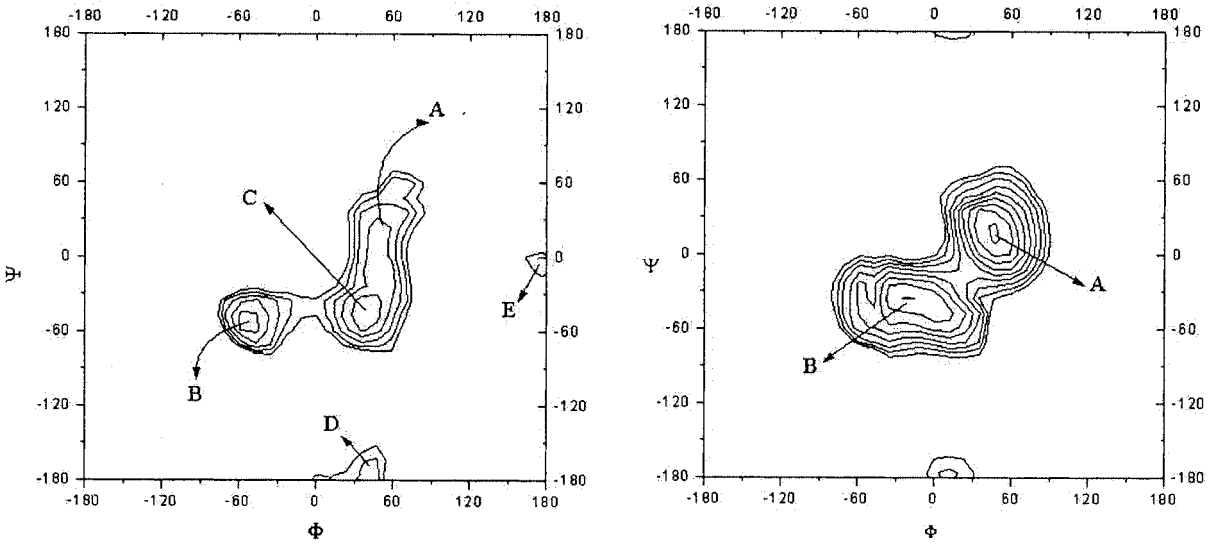

Figure 2. Potential energy maps based on calculations with the MM3* force-field (GB/SA) solvent model for compounds **1** (left) and **2** (right); energy contours are given every 2 kJ/mol; the key conformers are marked; conformers D and E of **2** reach a rather high energy level and are not indicated here

Remarkably, differences between compounds **1** and **2** in their conformational behavior are pronounced. The data from simulations are conspicuously similar to the probability distributions obtained by the systematic molecular mechanics approach. Again, for compound **1**, the MM3*-based MD simulations (Figure 3) predict the predominant presence of the 60°/−60° conformer, with additional contributions from the −60°/−60° and 60°/60° geometries. Minor sampling of the *anti*-Φ and *anti*-Ψ regions is also observed. The results of the AMBER*-based MD simulations basically arrive at the same conclusion.

In the case of compound **2**, the results of MD simulations both with the MM3* and with the AMBER* force-fields are similar to the results of the systematic approach. Use of both force-fields independently produces an equilibrium between a major (ca. 90%, *exo*-Φ/Ψ$_+$) and a minor, non-*exo*-anomeric conformer with access to about 10% of the total population area (Figure 3).

The conformational space having at this stage been described by modeling, it was next of interest to characterize the conformational behavior of the compounds experimentally. As well as giving analytical insights into these sub-

Table 2. Expected distances estimated from the molecular mechanics (MM) and molecular dynamics simulations (MD) for the two low-energy conformers of compound **2**; the range is the result of the MM3* and AMBER* calculations; the key distances and NOEs are given in bold-italic; collected average distances together with the calculated NOEs based on a full-matrix relaxation approach in comparison with the intensities of the observed NOEs are also given

Proton pair	Conformer A *exo*-Φ/Ψ_+ Expected distances MM	Conformer B Non-*exo*-Φ/Ψ_- Expected distances MM	Ensemble average MM3* Distances MM	MD simulations MM3* and AMBER* Distances MD	Ensemble average MM3* Calculated NOEs	Observed intensity for NOEs (500 MHz)[a]
H1′−H3	4.4−4.5	3.4−3.6	4.4	3.4−4.2	0−1%	not observed
H1′−H4	2.4−2.5	2.3−2.6	2.4	2.4−2.5	9−11%	overlap
H1′−H6a	2.3−2.4	4.2−4.5	2.6	2.4−3.0	2−5%	+++
H1′−H6b	3.5−3.9	5.5−5.7	3.6	3.1−3.6	0−1%	+
H7′eq−H3	4.2−4.3	3.0−3.4	4.0	3.0−3.8	0−1%	+
H7′eq−H4	2.2−2.3	4.0−4.3	2.4	2.3−2.7	8−15%	++++
H7′eq−H5	4.8−4.9	4.6−4.8	4.8	3.8−4.8	0	not observed

[a] For intensity grading, please see footnote to Table 2.

stances, this comparison should also broaden the basis for gauging the quality of the modeling procedures.

NMR Spectroscopy of the Synthetic Compounds Free in Solution

In the first step of our NMR experiments, the complete set of resonance signals was determined. The chemical shifts of **1** and **2** in D_2O are listed in Table 2 in the Supporting Information. The assignment of the resonances was achieved through a combination of COSY, TOCSY, 1D- and 2D-NOESY/ROESY, and HSQC experiments (Figure 4 and Supporting Information).

The *J* values for the ring protons supply the information that pyranose chairs adopt the usual $^4C_1$ chair forms, irrespective of the size of the molecule and of the nature of the C-glycosidic linkage. Thus, any presence of alternative chair conformations, as described for other C-glycosyl compounds,[16] is undetectable. The intermediate observed values for the C5−C6 lateral chains are in agreement with equilibria between the tg:gt conformers for the pseudoGal rings and the gg:gt conformers for the Glc moieties.

In the second set of NMR experiments, NOESY and ROESY measurements were carried out in order to obtain the relevant conformational information. The intensities of the observed NOEs in relation to those estimated by the MM3*- and AMBER*-based molecular mechanics and molecular dynamics calculations, by a full relaxation matrix approach, are also presented in Tables 1 and 2. The assessment of the conformational behavior of **1** was facilitated by analysis of the measured interglycosidic *J* values between the prochiral methylene protons and the H-1′ and H-4 protons at the glycosidic and aglyconic positions. In particular, for **1**, as shown in Table 3, the observed $J_{\mathrm{HproS-H1'}}$ and $J_{\mathrm{HproS-H4}}$ scalar couplings are small, indicating that the corresponding major populations of conformers around these proton-proton torsions are *syn*. In contrast, the $J_{\mathrm{HproR-H1'}}$ and $J_{\mathrm{HproR-H4}}$ coupling constants show large values, clear evidence for the predominance of conformers with a major *anti* orientation between these two proton pairs.

By consideration of the basic conformers around both torsions, an equilibrium with a 90:5:5 distribution between the *exo* (D + C + A)/*anti* (E)/non-*exo* (B) staggered conformers around Φ and a 5:85:5:5 distribution between the four possible conformers Ψ_+(A)/Ψ_-(B + C)/eclipsed-Ψ(E)/*anti*-Ψ(D) around Ψ match the observed coupling characteristics in a satisfactorily quantitative manner. Therefore, from the analysis of coupling constants and consideration of the geometries derived from molecular mechanics calculations, the relative extents of population in regions A−E should be around 5, 5, 80, 5, and 5%, respectively. The relative population of conformer B (non-*exo*-anomeric) thus appears to be overestimated by the MM3* simulations.

These semiquantitative observations were further extended and corroborated by NOE measurements (Figure 4). For **1**, the simultaneous presence of a number of exclusive NOEs in different conformers cannot be explained in terms of a single conformer or even an equilibrium between two conformers. The presence of NOEs (Tables 1 and 2) originating from the proton pairs H3−HproR, H5−HproR, H1′−H4, and HproS−H6a indicates that the 60°/−60° (*exo*-Φ/Ψ_-) conformer should indeed be abundantly present in solution. Fittingly, this conformational property explains the simultaneous presence of all the NOEs mentioned above. Furthermore, the presence of weak H3−HproS and H5−HproS NOE contacts demonstrates population of further conformational positions in equilibrium. Indeed, a minor proportion of the accessible conformational space attributable to the *exo*-Ψ_+ appears to account for occurrence of these contacts. No exclusive NOEs allowing the presence of non-*exo* conformers to be detected unambiguously are observed, although the MM3* and AMBER* force-field calculations predict their contribution in solution. The experimental data further detect the slight presence of *anti*-Φ and *anti*-Ψ conformers, in the form of very weak NOEs between H2′−H4, exclusive to *anti*-Φ, and of H1′−H3 and H1′−H5 NOEs, indicative of *anti*-Ψ conformations. In aggregate, the agreement between the theoretical NOEs obtained from the full-matrix relaxation analysis, from the molecular mechanics and molecular dy-

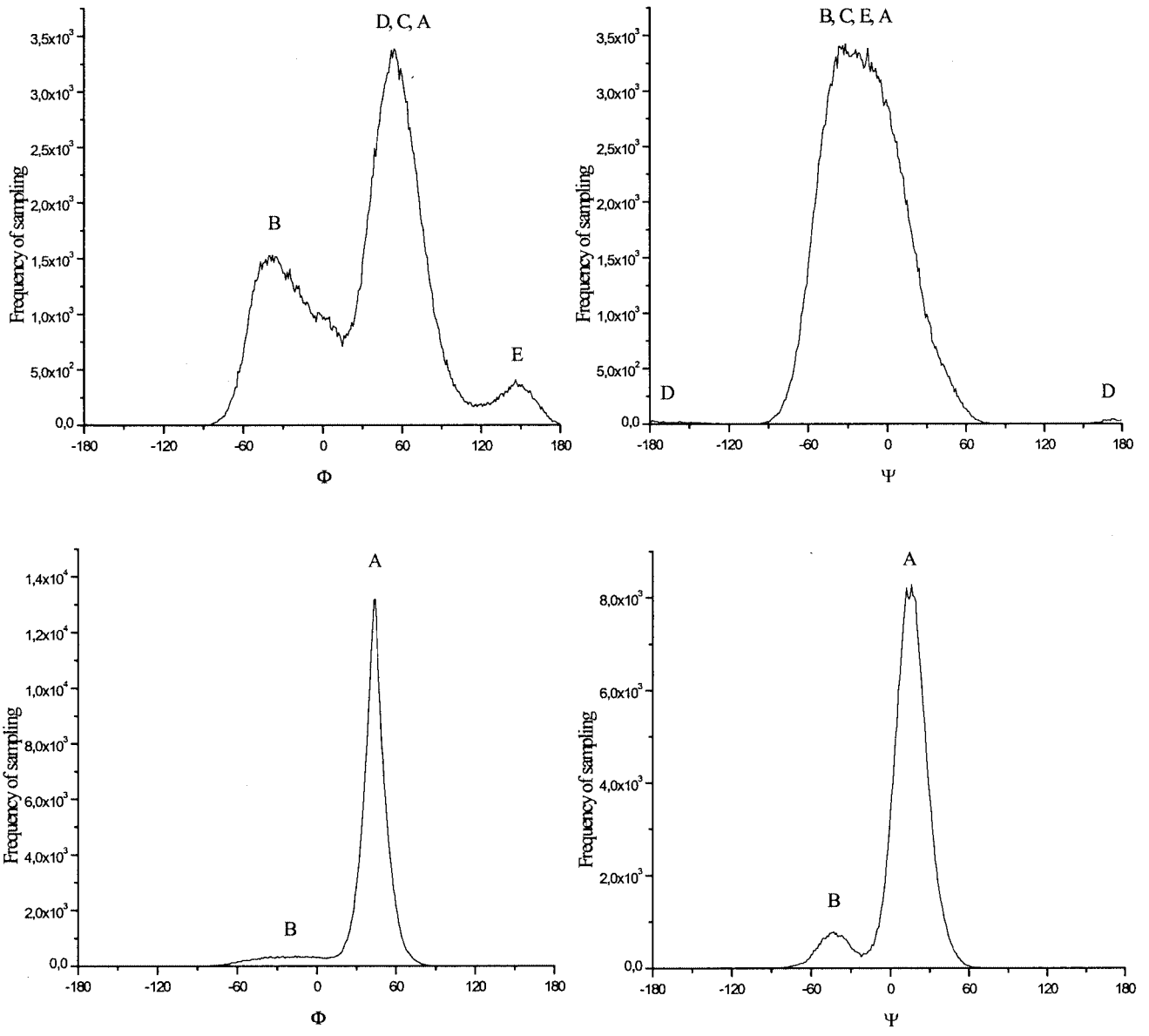

Figure 3. Frequency of sampling of Φ/Ψ torsion angles from the MD simulations (MM3* force-field) for compounds **1** (top) and **2** (bottom); the superimposition resulting from MD runs for a period of 12.5 ns (for **1**) and 5 ns (for **2**), respectively, is shown; the torsion angle values for the different conformers are indicated

namics calculations, and from the experimentally observed NOEs is more than satisfactory. Therefore, after consideration of the *J*- and NOE-based information, the lesson that emerges is that compound **1** is subject to major conformational averaging around the Φ and Ψ glycosidic linkages with fairly likely participation of five conformers in the conformational equilibrium, with fairly small energy barriers between them. This behavior is in marked contrast with that of lactose (**3**).[17]

The analysis of the conformational behavior of compound **2** free in solution was solely based on NOEs. Here, a significant conformational difference with respect to **1** could be seen. The presence of the intense and exclusive H7eq−H4 NOE, together with the observation of the H1′−H6a contact, allowed the presence of a major 60°/60° (*exo*-Φ/Ψ_+) conformation to be deduced. The presence of *anti*-Φ or *anti*-Ψ conformers appeared to be almost negligible, because H2′−H4, H1′−H3, and H1′−H5 NOEs were below the noise levels in both NOESY and T-ROESY experiments at various mixing times, notably in line with results of the molecular mechanics calculations. Furthermore, detection of a weak NOE between H7eq−H3 suggests the presence of a minor proportion of the non-*exo*-Φ/Ψ_- conformer. The agreement between the expected (from MM and MD calculations) and the experimentally observed NOEs is, as noted above, satisfactory. The conformational behavior of **2** therefore appears to be represented by a distribution between a major (*exo*-Φ/Ψ_+) and a minor conformer (non-*exo*-Φ/Ψ_-), squaring well with the results of the MD simulations as presented in Figure 3.

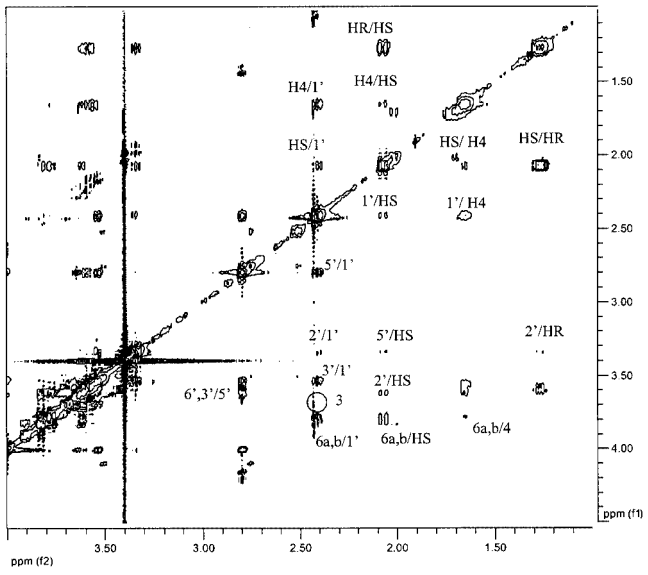

Figure 4. T-ROESY spectrum (mixing time 400 ms) of **1** carried out at 500 MHz, pH = 7 and 300 K; key cross-peaks are indicated

30:5:10:50:5, with a higher population attributable to the *anti*-Ψ region at the expense of the *syn*-Ψ section. Given the structural similarities between the two compounds, the difference in polar interactions of the N vs. the O atoms in the *syn*-Ψ and the *anti*-Ψ regions should contribute to an explanation of the observed conformational differences (a 45% conformational population shift between both regions). There are also differences in the population density of regions A−E for glycomimetic **2** versus the natural compound **3** (90:10:< 5:< 5:< 5 for **2** vs. 90:< 5:< 5:10:< 5 for **3**). The observed conformational disparities should be stereoelectronic in origin. If it is assumed that the steric interactions at the glycosidic (C−O−C) linkages of **2** and **3** are similar, it is possible to estimate the stereoelectronic contribution of the *exo*-anomeric effect qualitatively. Compound **2**, without *exo*-anomeric stabilization, presents a ca. 90:10 proportion of *exo*/non-*exo* conformers around Φ, while natural lactose (**3**), with *exo*-anomeric stabilization, shows an almost exclusive predominance of *exo* conformers (ca. 99:1). Therefore, qualitatively, the corresponding stabilization due to the stereoelectronic contribution of the *exo*-

Table 3. Expected *J* values [Hz] for the basic conformations around Φ and Ψ angles for **1**, deduced by application of the generalized Karplus equation proposed by Altona to the geometries provided by MM3* and AMBER* molecular mechanics calculations; the distribution of relative population of 90:5:5 over the three (*exo*, *anti*, non-*exo*) conformers around Φ and of 5:85:5:5 over the four conformers (Ψ_+,Ψ_-, eclipsed-Ψ, *anti*-Ψ) around the Ψ angle in the equilibrium match the observed couplings in an almost quantitative manner

Proton pair	Conformer					
	exo-Φ	*anti*-Φ	non-*exo*-Φ		AVERAGE	Exp. Sect.
H1′−HproS	1.0−1.4	5.0	11.2−11.5		1.9	2.0
H1′−HproR	10.8−11.3	1.9	3.2−4.0		10.2	9.5
	Ψ_+	Ψ_-	eclipsed-Ψ	*anti*-Ψ		
H4−HproS	9.0−12.4	2.0−2.5	4.7	2.9−3.3	2.8	2.6
H4−HproR	1.4−2.5	12.3−12.4	4.3	3.8−4.1	1.0	8.0

Comparison of the Conformational Behavior of Compounds 1 and 2 in the Free State with that of Lactose (3) and C-Lactose (4)

The combination of molecular mechanics calculations and NMR experiments has guided us to the conclusion that compound **1**, with a methylene group at the pseudoglycosidic position, exhibits a higher degree of flexibility than compound **2**, possessing an oxygen atom in that position, although it also lacks the *exo*-anomeric effect. The difference between C−C (ca. 1.54 Å) and C−O (ca. 1.41 Å) distances, together with the variation in the bond angles (C−O−C vs. C−C−C), is fairly probably a major factor in this difference in conformational behavior. In summary, compound **1** shows a relative distribution of ca. 5:5:80:5:5 over the conformers A−E, while the relative distribution in the conformational equilibrium of its closely related analogue, C-lactose (**4**), with an endocyclic oxygen atom at the galactose moiety instead of the nitrogen atom in **1** is ca. anomeric effect amounts to ca. 1.9 kcal/mol.[18] On the other hand, calculation of these relatively small energy barriers between the different conformational regions for both lactose analogues intimates that conformers other than the major one coexist in solution. Carbohydrate-binding proteins such as lectins ("locks") might select any of the present shapes or only distinct ones ("keys") without severe steric/thermodynamic conflicts. It has previously been reported that C-glycosides and carbaglycosides are able to bind to glycosidases and a few studied lectins.[9,18−20] Notably, even very minor conformers can serve as preferred ligands. Significantly in this respect, *E. coli* β-galactosidase selects the high-energy *anti* conformation of the C-glycosyl analogue of lactose.[19] Interestingly, although this enzyme also selects a high-energy conformation of the natural compound, lactose, the nature of the conformational distortion is different. In the C-glycosyl analogue, the enzyme rotates Φ in 120° from the low-energy state value. In contrast, and

for stereoelectronic reasons, the enzyme distorts the galactose chair of the natural compound.[20] The issue outlined above was resolved by use of a galactoside-specific lectin, as described in detail in the next part.

Lectin-Bound Conformations of the Synthetic Compounds

It having been observed by free-state analysis that the profiles of the solution behavior of **1** and **2** are different from that of the O-glycoside **3**, the glycomimetics were next confronted with mistletoe lectin in solution, and the mixture was scrutinized by NMR spectroscopy. As noted at the end of the last paragraph, depending on the topology of the receptor's binding site, conformer accommodation with and without selection can take place. The mistletoe lectin primarily homes in on the galactose moiety, as documented by a detailed analysis of its carbohydrate specificity including mapping with lactose derivatives.[1c,21] To collect evidence for an actual interaction between the compounds and the lectin − that is, ligand properties of the synthetic compounds − 1D ^{1}H NMR spectra were recorded after addition of the lectin to the NMR tubes containing **1** or **2** dissolved in a D_2O-based phosphate buffer (Figure 4 in the Supporting Information).

The presence of the lectin caused significant line-broadening of the glycosyl signals, thus providing a clear indication of binding. Therefore, in a further step to identify the conformational features of the bound ligand, TR-NOESY[22] spectra were recorded. TR-NOE cross-peaks of negative sign were observed for the complexes forming between both analogues and VAA. They are characteristic for the bound state of a ligand. The corresponding NOE cross-peaks were weak and positive for the free compounds. The negative cross-peaks in the TR-NOESY convey conformational information relating to the bound glycomimetic. The spectra shown in Figures 5 and 6 illustrate the signal pattern for complexes containing compounds **1** and **2**, respectively. Comparison of these sets of NOE cross-peaks, at several mixing times, indicated that both patterns of the signals differ from those observed in the free state (compare Figures 5 and 6 vs. Figure 4).

In detail, several signals detected in the free-state conformational profile no longer appear in the spectra of the complexes. Apparently, ligand binding restricts the accessible conformational space, a clear indication of conformer selection [i.e., only one or a limited set of conformers of the complete set present in the free state is (are) bound by this lectin]. The observed TR-NOEs are listed in Table 4, along with their representative conformers. As a reminder, important exclusive NOEs for **1** are H1′−H4 (conformers B and C), H1′−H3, HproR−H6a and H1′−H5 (conformer D), and H2′−H4 (conformer E). As noted above, there is no exclusive NOE for the non-*exo*-anomeric conformer B.

With further scrutiny of the information in the spectra for **1** as ligand, the observed cross-peaks (Figure 5) indicate intramolecular mobility of the ligand in the bound state. The simultaneous presence of exclusive NOEs characteristic for different conformers [i.e., H1′−H4 (*syn*-Φ), H1′−H3 (*anti*-Ψ), and H2′−H4 (*anti*-Φ) NOE cross-peaks; Table 1],

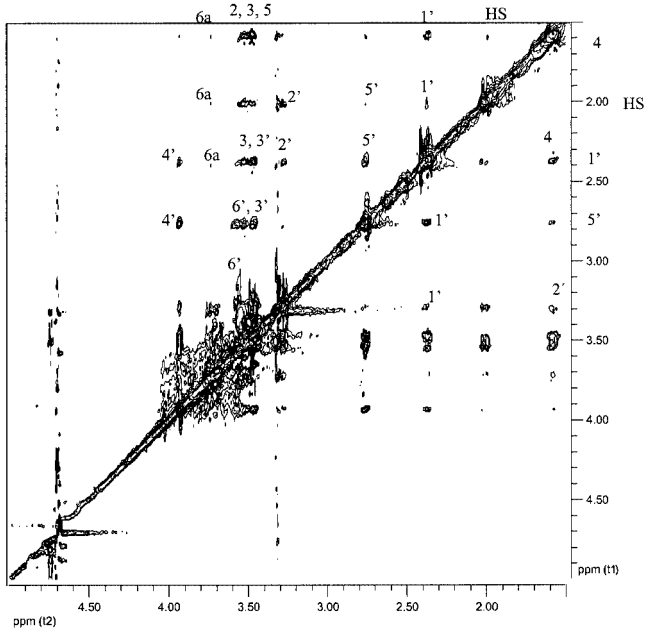

Figure 5. TR-NOESY spectrum (mixing time 200 ms) of **1** in the presence of the mistletoe lectin (25:1 molar ratio), carried out at 500 MHz, pH = 7 and 300 K; key cross-peaks are indicated

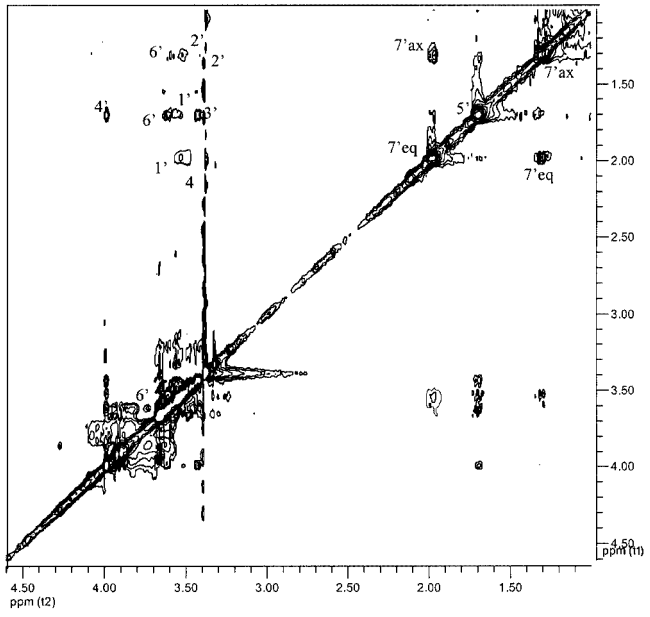

Figure 6. TR-NOESY spectrum (mixing time 200 ms) of **2** in the presence of the mistletoe lectin (34:1 molar ratio), carried out at 500 MHz, pH = 7 and 300 K; key cross-peaks are indicated

argues in favor of the ligand still harboring a certain degree of flexibility. A quantitative analysis by the full relaxation matrix approach was performed . However, it was not possible to match the cross-peaks reliably for both sides of the glycosidic linkages with a single correlation time. In view of the lack of complete ligand immobilization within the binding site, different proton pairs may well have different effective correlation times, a likely explanation for why this procedure did not work satisfyingly. In addition, contact to the

Table 4. Observed NOEs for the key proton pairs of compound **1** in the free state and in the presence of mistletoe lectin (VAA)

Proton pair	Observed intensities (bound state)[a]	Observed intensities (free state)[a]	Proton pair	Observed intensities (bound state)	Observed intensities (free state)
H1′−HR.	++	++	H4−H2,3,5	++++	++++
H1′−HS	+++	++++	H4−H6a,b	+++	+++
H1′−H4	+++	++++	H5−HR	not observed	+++
H1′−H5′	+++	+++++	H5′−H6′	+++	++++
H1′−H6a,b	++	+++	H5′−H3′	+++	+++++
H1′−H3	+++	++	H5′−H4′	++++	+++++
H1′−H3′	++++	+++++	HR−H6a,b	++	+
H2′−H4	++	+	HR−H6′a,b	+++	not observed
H1′−H5	not observed	+	HS−H6a,b	++	+++
H3−HR	++	+++	HS−H5′	++	not observed
H4−HR	++	++	HS−H2′	+++ to ++++	++++
H4−HS	++++	++++	HS−H5	+++	++

[a] For intensity grading, please see footnote to Table 2.

reducing-end moiety in disaccharides had been described as comparatively weak, explaining the clear preference of the mistletoe lectin for galactose as key epitope for binding.[7c,23] In aggregate, compound **1** is subject to a limited degree of conformer selection by the mistletoe lectin. In other words, intramolecular flexibility is still possible for lectin-bound ligands.

In the case of compound **2**, in contrast, there is unambiguous evidence for binding of the major *exo*-anomeric conformer of **2** by VAA, as indicated by the presence of the exclusive NOE of H7eq′−H4, which substantiates our conclusion. This behavior of **2** resembles that of natural lactose (**3**), when bound to VAA.[24] This lectin therefore appears to select *exo*-anomeric conformers of both **1** and **2** preferentially, although minor presence of conformer B in the bound state cannot be completely ruled out. Thus, the "natural" *exo*-anomeric conformers around the glycosidic angles of the pseudodisaccharides **1** and **2** are bound by VAA, and so these compounds in fact behave as true glycomimetics.

Conclusions

The combination of molecular mechanics calculations and NMR experiments permit the conclusion that lactose mimetics **1** (aza C-glycosyl compound) and **2** (carba analogue), lacking the *exo*-anomeric effect, resemble the natural counterpart − lactose (**3**) − in their conformational behavior, with somewhat higher flexibility. Nevertheless, all the conformations sampled by the natural compound are also accessible to these glycomimetics. TR-NOE experiments for these glycomimetics in the presence of mistletoe lectin have made it possible to demonstrate that the glycosidic angles of **1** can access a larger range of conformational space than those of the natural compound **3**, and its mimic **2**, when bound to VAA, for which only the regular *exo*-anomeric-type of conformation is bound. This observed conformational mobility also differs from that reported for C-lactose **4** when bound to the plant lectin ricin (B-chain),[25] to the growth-regulatory mammalian lectin galectin-1,[9] and also to *E. coli* β-galactosidase.[19] In all these cases, one distinct conformer is bound, and ligand accommodation precludes conformational averaging. This evidently different behavior of the **1**/VAA pair teaches that details of the chemical nature of the sugar ligand can markedly affect properties of the bound state, here flexibility. Disparities with structurally closely related compounds are thus possible, underscoring the value of systematic study of glycomimetics.

Experimental Section

Materials: The synthesis of these compounds has been described elsewhere.[26] The mistletoe lectin was purified by affinity chromatography on Sepharose 4B to which lactose had been attached after divinyl sulfone activation, and the purity and activity were routinely checked by 1D and 2D gel electrophoresis and by hemagglutination/cell binding/solid-phase assays, as described.[27]

Molecular Mechanics and Dynamic Calculations: Potential energy surfaces and population maps were calculated by use of the MM3* and AMBER* force-fields, as implemented in Macromodel 7.1.[28] The torsion angle Φ is defined as H1′−C1′−X−C4 and Ψ as C1′−X−C4−H4, where X is the atom in the glycosidic bridge. In the first step, a Φ/Ψ map was calculated by use of a grid step of 18° at each torsion coordinate. The corresponding 400 conformers were optimized by fixing the Φ/Ψ positions at each corresponding value to generate the relaxed energy map. The probability distribution was calculated from the energy values according to a Boltzmann function at 300 K. In the molecular mechanics and molecular dynamics calculations, the GB/SA solvation model for water was invariably used. Molecular dynamics simulations were also performed with both MM3* and AMBER* force-fields in Macromodel 7.1. For molecular dynamics simulations, several geometries corresponding to the different low-energy minima were used as input. A simulation temperature of 300 K was employed with a time step of 1.5 fs and an equilibration time of 100 ps. The total simulation times for each compound were 10 ns for **1** (four starting conformations) and 5 ns for **2** (two starting conformers).

NMR Spectroscopy: 500 MHz ^{1}H NMR spectra were recorded at 30 °C in D_2O with Varian Unity and Bruker DRX 500 NMR spectrometers. Concentrations of **1** and **2** of 5 mM were used. Chemical shifts are reported in ppm, with external TMS ($\delta = 0$ ppm) as reference. The 2D-TOCSY experiment (70 ms mixing time) was generally performed by use of a data matrix of 256 × 2 K to digitize a spectral width of 3000 Hz. Four scans were used per increment with a relaxation delay of 2 s. 2D-NOESY (300, 400, and 500 ms) and 2D-T-ROESY experiments (300 and 400 ms) used the standard sequences; 1D-selective NOE spectra were acquired by use of the double echo sequence proposed by Shaka and co-workers[29] at five different mixing times (200, 400, 600, 800, and 1000 ms). NOESY back-calculations were performed as described. The calculations to obtain theoretical NOEs were automatically performed with the aid of a home-made program, available from the authors upon request.[20,30] TR-NOE experiments with the mistletoe lectin as receptor were performed at 500 MHz. The lectin was first subjected to two cycles of lyophilization with D_2O as solvent to remove traces of H_2O and transferred in solution to the NMR tube to give a final concentration of ca. 0.1−0.2 mM. TR-NOESY experiments were performed with mixing times of 150, 200, and 250 ms, for molar ratios between 17:1 and 34:1 of the compounds relative to the lectin. No purging spin lock period to remove the protein signal background was employed. In all cases, the line-broadening of the sugar protons was monitored first after the addition of the ligand. The theoretical analysis of the TR-NOEs of the sugar protons was performed by use of a relaxation matrix with exchange, as described.[9,19,25] Different exchange-rate constants (k) and leakage relaxation times were tested in order to reach an optimal match between experimentally obtained and theoretically predicted results for the intraresidual H1−H2 cross-peaks of the reducing moiety for the given protein/ligand ratio. Normalized intensity values were used since they allow correction for spin-relaxation effects. The overall correlation time τ_c for the free state was always set to 0.15 ns and τ_c for the bound state for VAA was estimated at 40 ns. To fit the experimental TR-NOE intensities, different exchange-rate constants were tested, with external relaxation times ρ^* for the bound state of 0.5, 1 and 2 s. T-ROESY experiments were also carried out to exclude spin-diffusion effects. A continuous wave spin lock pulse was used during the 150 ms mixing time. Key NOEs were shown to be direct cross-peaks, because they revealed a different sign relative to the diagonal peaks.

Acknowledgments

The groups in Madrid sincerely thank the Ministry of Science of Technology of Spain for financial support (grants BQU2000-1501-C02 and BQU2003-03550-C03). M. C. F. A. is indebted to the Ministry of Education and Culture of Spain for a Ph.D. fellowship. The research at Hunter College was supported by the National Institutes of Health (NIH), General Medical Sciences (GM 57865) and a Research Centers in Minority Institutions (RCMI) award (RR-03037) from the National Center for Research Resources of the NIH. Funding from the EU (HPRN-CT20002-00173, Glycidic scaffolds) is also acknowledged.

[1] [1a] *Glycosciences: Status and Perspectives* (Eds.: H.-J. Gabius, S. Gabius), Chapman & Hall, London − Weinheim, **1997**. [1b] G. Reuter, H.-J. Gabius, *Cell. Mol. Life Sci.* **1999**, *55*, 368−422. [1c] H. Rüdiger, H.-C. Siebert, D. Solís, J. Jiménez-Barbero, A. Romero, C.-W. von der Lieth, T. Diaz-Mauriño, H.-J. Gabius, *Curr. Med. Chem.* **2000**, *7*, 389−416. [1d] H.-J. Gabius, S. André, H. Kaltner, H.-C. Siebert, *Biochim. Biophys. Acta* **2002**, *1572*, 165−177.

[2] [2a] Z. J. Witczak, *Curr. Med. Chem.* **1999**, *6*, 165−178. [2b] H. Driguez, *Top. Curr. Chem.* **1997**, *187*, 85. [2c] H. Yuasa, H. Hashimoto, *Rev. Heteroat. Chem.* **1999**, *19*, 35. [2d] N. Yamazaki, S. Kojima, N. V. Bovin, S. André, S. Gabius, H.-J. Gabius, *Adv. Drug Deliv. Rev.* **2000**, *43*, 225−244. [2e] D. Solís, J. Jiménez-Barbero, H. Kaltner, A. Romero, H.-C. Siebert, C.-W. von der Lieth, H.-J. Gabius, *Cells Tissues Organs* **2001**, *168*, 5−23. [2f] B. G. Davis, M. A. Robinson, *Curr. Opin. Drug Discov. Develop.* **2002**, *5*, 279−288.

[3] For instance, see: [3a] R. V. Weatherman, L. L. Kiessling, *J. Org. Chem.* **1996**, *61*, 534−538. [3b] R. V. Weatherman, K. H. Mortell, M. Chervenak, L. L. Kiessling, E. J. Toone, *Biochemistry* **1996**, *35*, 3619−3624. [3c] L. M. Mikkelsen, M. J. Hernáiz, M. Martín-Pastor, T. Skrydstrup, J. Jiménez-Barbero, *J. Am. Chem. Soc.* **2002**, *124*, 14940−14951.

[4] [4a] M. S. Searle, D. H. Williams, *J. Am. Chem. Soc.* **1992**, *114*, 10690−10697. [4b] H.-J. Gabius, *Pharmaceut. Res.* **1998**, *15*, 23−30. [4c] T. K. Dam, C. F. Brewer, *Chem. Rev.* **2002**, *102*, 387−429.

[5] [5a] W. Levy, D. Chang, *Chemistry of C-Glycosides*, Elsevier, Cambridge, UK, **1995**. [5b] J. Jiménez-Barbero, J. F. Espinosa, J. L. Asensio, F. J. Cañada, A. Poveda, *Adv. Carbohydr. Chem. Biochem.* **2001**, *56*, 235−284.

[6] [6a] R. U. Lemieux, S. Koto, D. Voisin, *Am. Chem. Soc., Symp. Ser.* **1979**, *87*, 17−29. [6b] A. J. Kirby, *The Anomeric Effect and Related Stereoelectronic Effects at Oxygen*, Springer-Verlag, Heidelberg, Germany, **1983**. [6c] I. Tvaroska, T. Bleha, *Adv. Carbohydr. Chem. Biochem.* **1989**, *47*, 45−103. [6d] G. R. J. Thatcher, *The Anomeric Effect and Associated Stereoelectronic Effects*, American Chemical Society, Washington, DC, USA, **1993**.

[7] [7a] H. Kaltner, B. Stierstorfer, *Acta Anat.* **1998**, *161*, 162−179. [7b] A. V. Timoshenko, I. V. Gorudko, H. Kaltner, H.-J. Gabius, *Mol. Cell. Biochem.* **1999**, *197*, 137−145. [7c] H. Rüdiger, H.-J. Gabius, *Glycoconjugate J.* **2001**, *18*, 589−613.

[8] [8a] H.-J. Gabius, F. Darro, M. Remmelink, S. André, J. Kopitz, A. Danguy, S. Gabius, I. Salmon, R. Kiss, *Cancer Invest.* **2001**, *19*, 114−126. [8b] H.-J. Gabius, *Biochimie* **2001**, *83*, 659−666. [8c] A. V. Timoschenko, Y. Lan, H.-J. Gabius, P. K. Lala, *Eur. J. Cancer* **2001**, *37*, 1910−1920. [8d] S. Gabius, H.-J. Gabius, *Dtsch. Med. Wochenschr.* **2002**, *127*, 457−459.

[9] For instance, see J. L. Asensio, J. F. Espinosa, H. Dietrich, F. J. Cañada, R. R. Schmidt, M. Martín-Lomas, S. André, H.-J. Gabius, J. Jiménez-Barbero, *J. Am. Chem. Soc.* **1999**, *121*, 8995−9000.

[10] N. L. Allinger, Y. H. Yuh, J. H. Lii, *J. Am. Chem. Soc.* **1989**, *111*, 8551−8559.

[11] D. A. Pearlman, D. A. Case, J. W. Caldwell, W. S. Ross, T. E. Cheatham, S. DeBolt, D. Ferguson, G. Siebal, P. A. Kollmann, *Comp. Phys. Commun.* **1995**, *91*, 1−41.

[12] For instance, see: [12a] A. Poveda, J. L. Asensio, T. Polat, H. Bazin, R. J. Linhardt, J. Jiménez-Barbero, *Eur. J. Org. Chem.* **2000**, 1805−1813. [12b] E. Montero, A. García-Herrero, J. L. Asensio, K. Hirai, S. Ogawa, F. Santoyo-González, F. J. Cañada, J. Jiménez-Barbero, *Eur. J. Org. Chem.* **2000**, 1945−1952, and references cited therein.

[13] [13a] J. L. Asensio, J. Jiménez-Barbero, *Biopolymers* **1995**, *35*, 55−71. [13b] J. L. Asensio, M. Martín-Pastor, J. Jiménez-Barbero, *J. Mol. Struct. (THEOCHEM)* **1997**, *395*, 245−270.

[14] For a discussion on the application of molecular mechanics force-fields to sugar molecules, see: S. Pérez, A. Imberty, S. B. Engelsen, J. Gruza, K. Mazeau, J. Jiménez-Barbero, A. Poveda, J. F. Espinosa, B. P. van Eijck, G. Johnson, A. D. French, M. L. C. E. Kouwijzer, P. D. J. Grootenhuis, A. Bernardi, L. Raimondi, H. Senderowitz, V. Durier, G. Vergoten, K. Rasmussen, *Carbohydr. Res.* **1998**, *314*, 141−155.

[15] For instance, see: A. D. French, J. W. Brady, "Computer Modelling of Carbohydrate Molecules", *ACS Symp. Ser.* **1990**.

[16] M. Carpintero, A. Bastida, E. García-Junceda, J. Jiménez-Bar-

bero, A. Fernández-Mayoralas, *Eur. J. Org. Chem.* **2001**, 4127−4135.
[17] J. L. Asensio, F. J. Cañada, J. Jiménez-Barbero, *Eur. J. Biochem.* **1995**, *233*, 618−630.
[18] J. L. Asensio, F. J. Cañada, N. Kahn, D. A. Mootoo, J. Jiménez-Barbero, *Chem. Eur. J.* **2000**, *6*, 1035−1041.
[19] J. F. Espinosa, E. Montero, A. Vian, J. L. Garcia, H. Dietrich, R. R. Schmidt, M. Martín-Lomas, A. Imberty, J. Cañada, J. Jiménez-Barbero, *J. Am. Chem. Soc.* **1998**, *120*, 1309−1316.
[20] A. García-Herrero, E. Montero, J. L. Muñoz, J. F. Espinosa, A. Vián, J. L. García, J. L. Asensio, F. J. Cañada, J. Jiménez-Barbero, *J. Am. Chem. Soc.* **2002**, *124*, 4804−4810.
[21] [21a] R. T. Lee, H.-J. Gabius, Y. C. Lee, *J. Biol. Chem.* **1992**, *267*, 23722−23727. [21b] O. E. Galanina, H. Kaltner, L. S. Khraltsova, N. V. Bovin, H.-J. Gabius, *J. Mol. Recognit.* **1997**, *10*, 139−147. [21c] S. André, P. J. Cejas Ortega, M. A. Perez, R. Roy, H.-J. Gabius, *Glycobiology* **1999**, *9*, 12583−1261. [21d] S. Bharadwaj, H. Kaltner, E. Y. Korchagina, N. V. Bovin, H.-J. Gabius, A. Surolia, *Biochim. Biophys. Acta* **1999**, *1472*, 191−196.
[22] J. Jiménez-Barbero, T. Peters (Eds.), *NMR Spectroscopy of Glycoconjugates*, Wiley-VCH, Weinheim, Germany, **2002**.
[23] M. Gilleron, H.-C. Siebert, H. Kaltner, C.-W. von der Lieth, T. Kozár, K. M. Halkes, E. Y. Korchagina, N. V. Bovin, H.-J. Gabius, J. F. G. Vliegenthart, *Eur. J. Biochem.* **1998**, *252*, 416−427.
[24] J. M. Alonso-Plaza, M. A. Canales, M. Jiménez, J. L. Roldán, A. García-Herrero, L. Iturrino, J. L. Asensio, F. J. Cañada, A. Romero, H.-C. Siebert, S. André, D. Solís, H.-J. Gabius, J. Jiménez-Barbero, *Biochim. Biophys. Acta* **2001**, *1568*, 225−236.
[25] J. F. Espinosa, F. J. Cañada, J. L. Asensio, M. Martín-Pastor, H. Dietrich, M. Martín-Lomas, R. R. Schmidt, J. Jiménez-Barbero, *J. Am. Chem. Soc.* **1996**, *118*, 10862−10871.
[26] [26a] X. Cheng, G. Kumaran, D. R. Mootoo, *Chem. Commun.* **2001**, 811−812. [26b] X. Cheng, N. Khan, G. Kumaran, D. R. Mootoo, *Org. Lett.* **2001**, *3*, 1323−1325.
[27] [27a] H.-J. Gabius, *Anal. Biochem.* **1990**, *189*, 91−94. [27b] S. André, R. J. Pieters, I. Vrasidas, H. Kaltner, I. Kuwabara, F.-T. Liu, R. M. J. Liskamp, H.-J. Gabius, *ChemBioChem* **2001**, *2*, 822−830. [27c] C. Unverzagt, S. André, J. Seifert, S. Kojima, C. Fink, G. Srikrishna, H. Freeze, K. Kayser, H.-J. Gabius, *J. Med. Chem.* **2002**, *45*, 478−491. [27d] L. He, S. André, H.-C. Siebert, M. Helmholz, B. Niemeyer, H.-J. Gabius, *Biophys. J.* **2003**, *85*, 511−524.
[28] F. Mohamadi, N. G. J. Richards, W. C. Guida, R. Liskamp, C. Caufield, G. Chang, T. Hendrickson, W. C. Still, *J. Comput. Chem.* **1990**, *11*, 440−467.
[29] K. Stott, J. Stonehouse, J. Keeler, T.-L. Hwang, A. J. Shaka, *J. Am. Chem. Soc.* **1995**, *117*, 4199−4200.
[30] J. F. Espinosa, M. Bruix, O. Jarreton, T. Skrydstrup, J.-M. Beau, J. Jiménez-Barbero, *Chem. Eur. J.* **1999**, *5*, 442−448.

Received October 27, 2003

